Chapter 3

Results

3.0 Results

3.1 Powder X-ray Diffraction

Powder X-ray diffraction is used to identify phases of crystalline material precipitated from aqueous molybdate solutions. One of the most interesting parts in varying all the preparation parameters is to observe the effect when temperature is varied while the other parameter is fixed because temperature will reveal significant difference to the precipitate by referring to other sets of parameters in this thesis (varying acid and molybdenum concentration). When ammonium and potassium are used as counter-ions at high temperature, hexagonal molybdenum oxide is obtained. The supramolecular structure can be recognised from the diffraction pattern when the peaks appear at lower angle and peaks are badly resolved with low intensity at higher angle. The results will be presented as a comparison between all sets of samples where only one parameter is varied while the other parameters are fixed.

3.1.1 Ammonium cation

Figure 3.1 shows an XRD pattern of samples prepared at the same concentration of AHM (0.7 M) and acid (1.0 M) but at different temperature (30 °C, 50 °C and 70 °C). Samples 256 and 232 precipitated spontaneously but sample 227 needed further heating. At 30 °C, a supramolecular phase is obtained while at 50 °C and 70 °C, hexagonal molybdenum oxide is obtained. It could be clearly seen that the pattern of supramolecular $Mo_{36}O_{112}^{4-}$ -like phase structure is accompanied by one sharp peak with high intensity. The peak appeared at approximately 7.0 ° in all supramolecular diffraction patterns. A few peaks at the 2 θ range 8-12 ° region appear with low intensity which are broad and accompanied by shoulders. There is also a trend whereby all samples show many small peaks which are badly resolved at 20-30 ° of 2 θ region which look like a growing peak with a little bit of high background. The pattern seems X-ray amorphous after approximately 40 ° and higher (no peak indicated at this region). Every sample of supramolecular $Mo_{36}O_{112}^{4-}$ phases show similar peak, which appear at approximately the same region. But obviously it is not the same phase because of the various characteristic of peak position, peak shape, peak width, presence of shoulder, and intensity. When temperature is set at 30 °C in all cases, the product precipitate spontaneously and supramolecular structure is obtained.

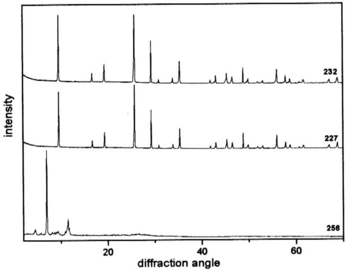

Fig 3.1 XRD pattern of 3 samples prepared at the same concentration of molybdenum (0.7 M) and acid concentration (1.0 M) but varying temperature; 256:30 °C, 227:50 °C and 232: 70 °

Figure 3.2 displays pattern of samples 257 and 228 with both having fixed concentration of molybdenum (1.0 M) and acid (1.0 M) but varying temperature, 30 °C and 50 °C, respectively. Both samples precipitated spontaneously. The interesting point is, even at 50 °C, spontaneous precipitation occurred as compared to sample 227, which does not show any spontaneous precipitation due to lower molybdenum concentration presence in the sample. It needed to be further heated to higher temperature and resulting in hexagonal molybdenum oxide being formed instead.

Thus, it can be concluded that spontaneous precipitation always results in supramolecular phase at lower temperature independent of acid and molybdenum concentrations (distributed randomly). When higher temperature is applied, hexagonal molybdenum oxide is yielded. Sample 248 (Figure A5, attached in Appendix A), however, did not precipitate spontaneously. In this case, the precipitate appeared at certain pH but re-dissolved and it needed to be further heated. After further heating, XRD revealed hexagonal molybdenum oxide phase.

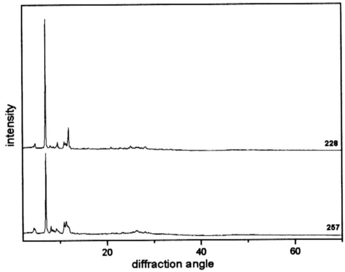

Fig 3.2 XRD patterns of 2 samples prepared at the same concentration of molybdenum (1.0 M) and acid concentration (1.0 M) but varying temperature; sample 257: 30 °C, sample 228: 50 °C.

More figures showing XRD patterns with many comparisons are attached in Appendix A. Those comparisons are plotted to indicate effect of preparation variables. In all cases, supramolecular $Mo_{36}O_{112}^{4-}$ phase was formed at low temperature independent of acid and molybdenum concentrations. As the temperature increased, the hexagonal molybdenum oxide phase was formed instead.

Most of the samples that were prepared at 50 °C did not precipitate spontaneously regardless of molybdenum and acid concentrations. Heating was required in order to obtain precipitation Heating was required in order to obtain which then enable the structure to be analysed. Table 3.1 shows a list of phase identified by XRD for all samples prepared using ammonium counter-ion at various temperature, acid and molybdenum concentrations.

Table 3.1 XRD phase identification of samples prepared using ammonium as counter-ion.

Sample Name	**[Mo] (M)**	**[H$^+$] (M)**	**Temperature (°C)**	**Phase**
256	0.7	1	30	Supramolecular-like phase
227	0.7	1	50	Hexagonal molybdenum oxide
232	0.7	1	70	Hexagonal molybdenum oxide
257	1	1	30	Supramolecular-like phase
228	1	1	50	Supramolecular-like phase
258	1	5	30	Supramolecular-like phase
248	1	5	50	Hexagonal molybdenum oxide
225	0.7	2	50	Supramolecular-like phase
223	1	2	50	Supramolecular-like phase

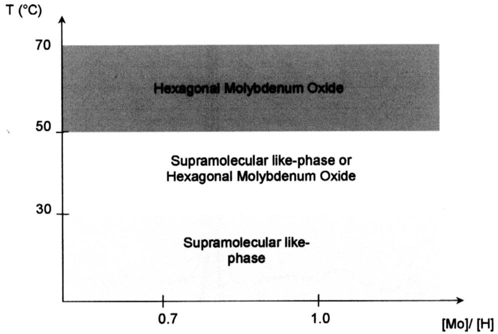

Fig 3.3 Diagram of state of phases yielded by varying parameters using ammonium as counter-ion

The effect of acid concentration, molybdenum concentration, and temperature changes to the product obtained can be presented in a plot of temperature as a function ratio of molybdenum to acid concentration shown in Figure 3.3. At 30 °C, supramolecular phase structure was yielded in all cases independent of acid and molybdenum concentration. Special cases at 50 °C whereby supramolecular and hexagonal phase yielded randomly independent of acid and molybdenum concentrations. At 70 °C, hexagonal phase was observed for all cases.

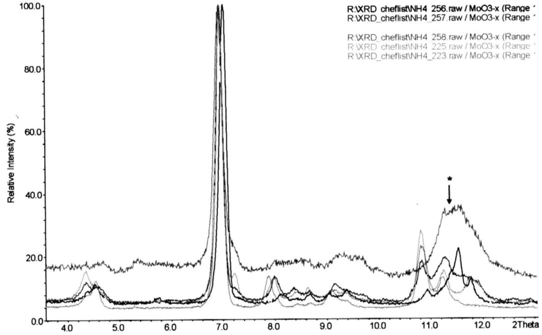

Fig 3.4 Section XRD patterns of samples with supramolecular phase structure prepared at various concentration of acid, concentration of molybdenum and temperature.

Figure 3.4 shows diffraction patterns of all supramolecular phase samples prepared at various acid concentrations, molybdenum concentrations and temperature. As can be clearly seen from the figure, none of the patterns are similar. All the samples have only one similarity, the peak occurs at approximately 7 ° 2 theta. Even this peak is slightly different from each other whereby the peak is accompanied by a small shoulder on the left and extra small peaks on the right. The most prominent difference was observed in sample 258 which is marked as *. This particular sample shows a pattern with higher background and relatively broader peak compared to the other patterns in the group.

One of the important difference is the position of the major peak of sample 256 which is shifted to higher angle (black line).

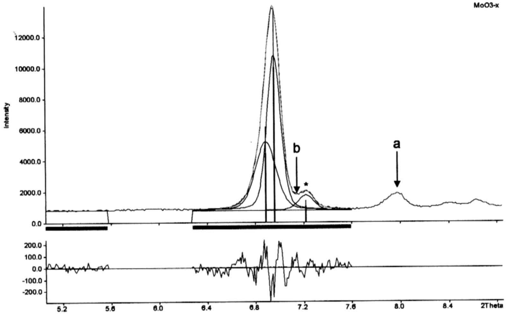

Fig 3.5 Peak fitting of characteristic peak of supramolecular phase, with minor peak on the left and major peak in the middle (corresponds to sample 225).

The single peak which always appeared at approximately 7.0 ° in every supramolecular diffraction pattern has been analysed further by calculating the d-spacing, and Full Width at Half Maximum (FWHM). The WinXPow ™ Software has been used to fit the peaks. The peaks were fitted by taking the single peak to have 2 peaks by looking at the shoulder (on the left side of every peak) which also appeared in all samples (Figure 3.5). The shoulder on the left side is called minor peak while the main peak is called major peak. The fit results in a low signal to noise ratio which is quite good.

In addition, the blue line (a) corresponds to the pattern of sample 225, while the green line (b) corresponds to combination of the fit and sample. Both lines overlapped with each other confirming that the fit is good enough. Small peak on the right side (*) is included into the fitting process in order to get a better fit. In principle, the purpose of adding the small peak on the right (*) and minor peak on the left is to get better fit for the major peak and to get a more accurate values of d-spacing and FWHM.

Table 3.2 Results of type of 2-peaks fitting, major peak

Sample Name	**[Mo] (M)**	**$[H^+]$ (M)**	**T (°C)**	**d-spacing (Å)**	**Angle**	**FWHM**	**Intensity (relative to major peak)**	**Remarks**
257	1.0	1.0	30	12.83	6.89	0.19	3 : 1	**
258	1.0	5.0	30	12.87	6.86	0.29	5 : 1	**
225	0.7	2.0	50	12.82	6.90	0.20	2 : 1	**
228	1.0	1.0	50	12.88	6.86	0.18	4 : 1	*
223	1.0	2.0	50	12.94	6.83	0.16	8 : 1	*
256	0.7	1.0	30	12.71	6.95	0.18	2.5 : 1	*

*fit with extra peak (on the right) to get better fit, total 3 peaks fit
** fit with only 2 peaks (no extra peak on the right), total 2 peaks fit

Table 3.3 Results of type of 2-peaks fitting, minor peak

Sample Name	**[Mo] (M)**	**[H$^+$] (M)**	**T (°C)**	**d-spacing (Å)**	**Angle**	**FWHM**	**Intensity**	**Remarks**
257	1.0	1.0	30	12.71	6.95	0.13	10637	**
258	1.0	5.0	30	12.74	6.93	0.17	3499	**
225	0.7	2.0	50	12.70	6.96	0.13	9981	**
228	1.0	1.0	50	12.74	6.93	0.12	18381	*
223	1.0	2.0	50	12.71	6.95	0.14	16541	*
256	0.7	1.0	30	12.60	7.03	0.12	11704	*

Table 3.2 and 3.3 show calculated d-spacing and FWHM of all supramolecular phase obtained from ammonium counter-ion resulted from peak fitting where both tables correspond to major peak and minor peak respectively. As can be seen in both Tables, the samples have been grouped into two. The first group was fitted with extra small peak on the right (marked as **) while the second group was fitted without it due to the absent of this small peak (marked as *). There is no real trend observed on the d-spacing and FWHM values. But the value of FWHM of sample 258 is significantly different for both major and minor peaks. As evidence from the pattern shown in Figure 3.4, the peak is relatively broader with higher background which explained the significant difference of half width in this pattern. In addition, sample 256 has the major peak shifted to the right resulted with the smallest d-spacing value, 12.71 Å. The d-spacing of this characteristic peak for other samples are in the range of 12.8 to 12.9 Å.

The type of hexagonal-molybdenum oxide structure is identified from the Powder Diffraction File (PDF-39-35) of Ammonia Molybdenum Oxide ($(NH_3)_3 MoO_3$), which provide the information for the hexagonal crystal system. This reference is confirmed by single crystal database (ICSD-38415). Besides the above references, two more references matched well with the characteristic pattern of hexagonal molybdenum oxide. These are references with PDF-file 29-115 which claimed hexagonal structure system and PDF-file 46-100 which claimed cubic structure (Table 3.4). The reference of PDF-file 39-35 was chosen as the right reference in agreement with single crystal reference, ICSD-38415.

Table 3.4 Possible references of molybdenum oxide.

Sample Name	**Chemical Formula**	**PDF File Number**	**Crystal System**	**Unit cell parameter**	
				a	**c**
Ammonium molybdenum oxide hydrate	$(NH_4)_{0.15} MoO_3$. $0.5H_2O$	29-115	hexagonal	6.09	9.14
Ammonium molybdenum oxide	$NH_3 (MoO_3)_3$	39-35 / ICSD-38415	hexagonal	10.57	3.73
Ammonium molybdenum oxide hydrate	$H_{0.68} (NH_4)_2 Mo_{14.16} O_{4.34}$. $6.92H_2O$	46-100	cubic	12.94	12.94

By applying peak fitting and unit cell refinement on these characteristic peaks based on reference (PDF-file 39-35), unit cell parameter of samples 227, 232 and 248 observed are shown in Table 3.5. The unit cell of all samples agreed quite well with reference. The *a* parameter are in the range of 10.56-10.58 Å while *c* parameter are almost similar with value approximately 3.73 Å.

Table 3.5 Comparison of unit cell parameter of samples with reference.

Sample Name	**Unit cell parameter**	
	a	**c**
227	10.570	3.728
232	10.564	3.729
248	10.575	3.729
PDF-file 39-35/ ICSD-38415	10.568	3.726

Figure 3.6 shows an XRD pattern of sample 227 with hkl value observed from reference (PDF-file 39-35). Investigation in more details revealed extra peak observed in most of the peaks at higher angle which appeared as a minor peak to the left of major peak. These peaks are believed to be the second hexagonal phase with different lattice parameter. One extra peak has been observed at 61.63 °. This characteristic peak is not in the pattern of the reference (PDF). By using the Powder Cell software, the hkl value has been calculated as (5, 1, 1).

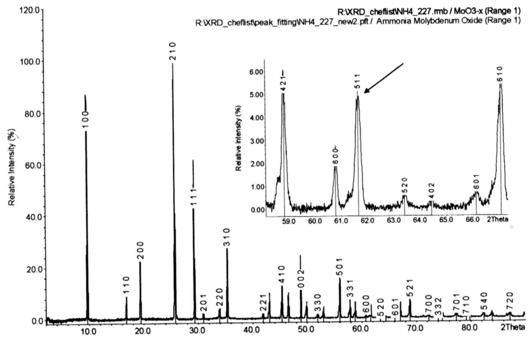

Fig 3.6 XRD pattern of sample 227 with hkl values.

3.1.2 Potassium cation

When Potassium is used as counter ion, 3 different structures have been observed, hexagonal potassium molybdenum oxide, supramolecular-like phase and trimolybdate. Figure 3.7 shows the influence of temperature using K_2MoO_4 (0.28 M) and HNO_3 (2 M). At 30 °C, the supramolecular phase was obtained spontaneously. At 50 °C and at 70 °C no immediate precipitation occurred. After further heating, hexagonal MoO_3 was obtained. Changing the acid concentration to 5 M yielded very similar results (see Figure A1-A20).

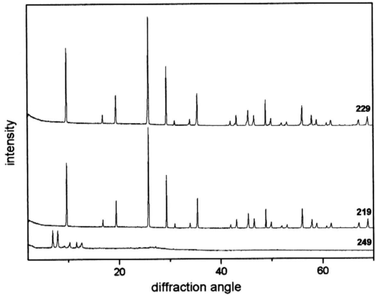

Fig 3.7 XRD pattern of 3 samples prepared at the same concentration of K_2MoO_4 (0.28 M) and HNO_3 (2.0 M) but varying temperature (sample 249:30 °C, 219:50 °C and 229:70 °C).

Further experiments investigating the temperature effect were carried out at different concentration using K_2MoO_4 (2 M) and HNO_3 (2 M). The resulting XRD patterns are shown in Figure 3.8. At all temperatures spontaneous precipitation appeared for all the different temperatures. At 30 °C and at 50 °C, a very ill defined supramolecular compound was obtained. The diffraction pattern is difficult to analyse and does not show a lot of similarities with the $Mo_{36}O_{112}^{4-}$ reference compound. At 70 °C a mixture of phases comprising trimolybdate as the major phase and at least one more additional minor phase was observed.

It is reported [45] that cation spaces, either occupied by H_3O^+, or K^+ depending on these crystal parameters will change. However it cannot be ruled out that more phases are also present. A similar result was obtained when the concentration of the acid was changed to 5 M. Again the supramolecular phase obtained was very ill defined, while on the other hand the trimolybdate was comparatively pure.

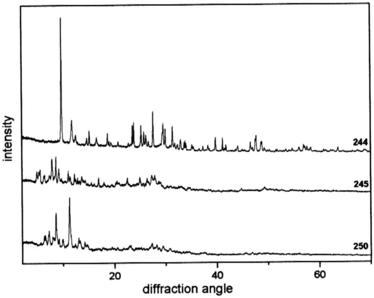

Fig 3.8 XRD pattern of 3 samples prepared at the same concentration of ·K_2MoO_4 (2.0 M) and HNO_3 (2.0 M) but varying temperature (sample 250:30 °C, 245:50 °C and 244:70 °C)

The influence of Mo concentration was also investigated. A spontaneous precipitation was achieved at low (0.28 M) as well as at high (2 M) Mo concentrations at 30 °C (comparison between sample 249 and 250).

In both cases, as usually observed earlier when samples precipitate spontaneously at low temperature, supramolecular compound was formed (see Figure A1-A10). When the same experiment was carried out at 50 °C, sample 219 with 0.28 M did not show spontaneous precipitation. However, sample 245 (2 M) still showed spontaneous precipitation with supramolecular-like phase. These series of experiments were carried out with 5 M HNO_3 as precipitating agent (sample 246). In principle the same results were obtained as with sample 245. Moreover the influence of varying acid concentration was checked.

Using similar procedure, the K_2MoO_4 solution at concentration of 2 M was chosen. A set of experiment with HNO_3 2 M and 5 M was carried out at 30 °C, 50 °C and 70 °C. The X-ray diffraction patterns of all products were identical for every set. At 30 °C and at 50 °C the supramolecular phase was produced. The experiment at 70 °C yielded the hexagonal potassium molybdenum oxide (see Figure A6-A19 in Appendix A).

More comparisons between each samples produced by potassium molybdate are presented in Figures A6-A19. The samples with hexagonal phase correspond to potassium molybdenum oxide hydrate with reference number of PDF-29-1022; ($K\ Mo_5\ O_{15}\ OH \cdot 2H_2O$). While trimolybdate which was observed in sample 243 and 244 corresponds to dipotassium catena-trimolybdate trihydrate with reference number of PDF-32-815, or ICSD-79413; ($K_2\ (Mo_3\ O_{10})\ (H_2\ O)_3$).

Table 3.6 shows the summary of phases produced using potassium as counter ion with various parameters. Overall, the series yielded supramolecular like-phase at low temperature and high K_2MoO_4 concentrations. Acid concentrations do not effect the phase formation. Trimolybdate was produced at high temperature and high molybdenum concentration and again acid concentration does not effect the phase formation. Moreover, hexagonal potassium molybdenum oxide was yielded at low concentration of K_2MoO_4 and high temperature.

Tab 3.6 Phase identification of samples prepared using potassium as counter-ion.

Sample Name	**[Mo] (M)**	**[H$^+$] (M)**	**Temperature (°C)**	**Phase**
249	0.28	2	30	Supramolecular like-phase
219	0.28	2	50	Hexagonal potassium molybdenum oxide
229	0.28	2	70	Hexagonal potassium molybdenum oxide
250	2	2	30	Supramolecular like-phase
245	2	2	50	Supramolecular like-phase
244	2	2	70	Trimolybdate
253	2	5	30	Supramolecular like-phase
246	2	5	50	Supramolecular like-phase
243	2	5	70	Trimolybdate
254	0.28	5	30	Supramolecular like-phase
247	0.28	5	50	Hexagonal potassium molybdenum oxide
233	0.28	5	70	Hexagonal potassium molybdenum oxide

The effect of acid concentration, K_2MoO_4 concentration, and temperature can be presented as a diagram of state in Figure 3.9 whereby perfect trends were observed. The product obtained by using ammonium as counter ion are independent of acid and molybdenum concentration and temperature, in contrast, potassium are influenced by temperature and molybdenum concentrations.

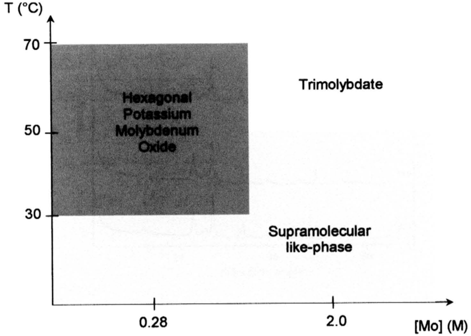

Fig 3.9 Diagram of state of phases yielded by varying parameters using potassium as counter-ion

3.1.3 Lithium cation

Using lithium as a counter ion did not produce any spontaneous precipitation (Figure 3.10). However, after heating the product was precipitated as molybdenum trioxide orthorhombic (PDF-file 5-508). Temperature variation was also found not influencing the obtained phase or crystallinity.

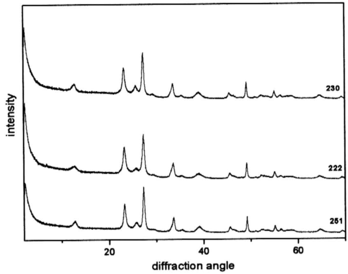

Fig 3.10 XRD pattern of 3 samples prepared at the same concentration of Li_2MoO_4 (0.28 M) and HNO_3 (2.0 M) and varying temperature (sample 251:30 °C, 222:50 °C and 230:70 °C) (need to be further heated).

Figure 3.11 shows an XRD pattern for sample 251 with hkl values taken from reference, PDF-5-508, MoO_3 orthorombic. Lithium samples showed XRD pattern with a mixture of sharp and broad peaks. Comparison on the hkl values taken from the PDF file, it is clear that the broad peaks are corresponding to the hkl values which are located along the b-axis, where Peak 1, Peak 2 and Peak 3 correspond to hkl values of (0, 2, 0), (0, 4, 0) and (0, 6, 0), respectively.

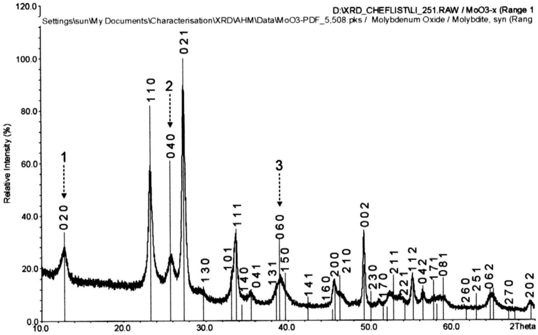

Fig 3.11 XRD pattern of sample 251 from Lithium cation with hkl value obtained from PDF 5-508, MoO₃ orthorombic.

3.1.4 Sodium cation

Finally the effect of sodium (Na) as counter ion was studied. For the temperature check, a Na_2MoO_4 solution of 2 M Mo was chosen with 2 M of HNO_3 as precipitation agent. The result is shown in Figure 3.12. Similar to earlier experiments, 30 °C, 50 °C and 70 °C were chosen and these correspond to sample 231, 226 and 252, respectively. To obtain precipitate all three samples needed further heating to 80 °C. After this, hexagonal molybdenum oxide was detected in all three samples with very similar diffraction patterns. The experiment exhibits similar result as when lithium was used as counter ion.

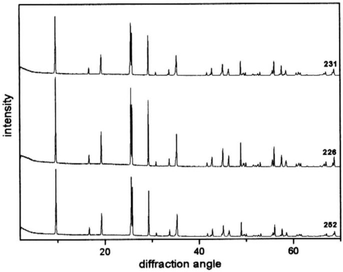

Fig 3.12 XRD pattern of 3 samples prepared at the same concentration of Na_2MoO_4 (0.28 M) and HNO_3 (2.0 M) and varying temperature (sample 251:30 °C, 222:50 °C and 230:70 °C).

This hexagonal phase corresponds to PDF 40-728 and ICSD 80289 with its chemical name, sodium molybdate water ($Na\,Mo_{5.33}\,H_{3.02}\,O_{18}\cdot 2H_2O$). Table 3.7 shows the summary of phases yielded when both lithium and sodium were used as counter ions. Both do not precipitate spontaneously until further heating is applied. Temperature does not affect the phase produced and also the crystallinity.

Tab 3.7 Phase identification of samples prepared using lithium and sodium as counter ions.

Sample Name	**[Mo] (M)**	**$[H^+]$ (M)**	**Temperature (°C)**	**Phase**
Lithium counter-ion				
0251	0.28	2	30	Orthorombic molybdenum trioxide
0222	0.28	2	50	Orthorombic molybdenum trioxide
0230	0.28	2	70	Orthorombic molybdenum trioxide
Sodium counter-ion				
0252	2	2	30 (further heated)	Hexagonal sodium molybdenum oxide
0226	2	2	50	Hexagonal sodium molybdenum oxide
0231	2	2	70	Hexagonal sodium molybdenum oxide
0255	2	5	30	Hexagonal sodium molybdenum oxide

3.2 Raman Spectroscopy

3.2.1 Phase Identification

Besides XRD analysis, the samples were investigated using Raman spectroscopy. The parameters were varied in the same way as in the XRD investigation. First the temperature effect was investigated. Ammonium heptamolybdate (AHM) solution 0.7 M and HNO_3 of 1 M were used. Figure 3.13 shows a sample of the result obtained from Raman Spectroscopy. The product obtained at 30 °C corresponds to sample 256 which shows bands at: 983, 959, 893, 848, 374 and 233 cm^{-1}. These bands are characteristic for the supramolecular compound [20]. The products obtained at 50 °C and at 70 °C correspond to sample 227 and 232, respectively and exhibit identical Raman spectra. Bands are situated at 976, 904, 887, 691, 494, 400, 256 and 225 cm^{-1}, indicating hexagonal MoO_3. Consequently Raman spectroscopy supports the XRD findings.

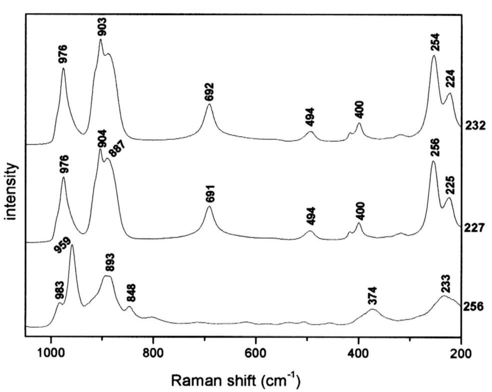

Fig 3.13 Raman spectrum of 3 samples prepared at the same concentration of AHM (0.7M) and HNO_3 (1.0 M) and varying temperature; 256:30 °C, 227:50 °C and 232: 70 °C.

Similar results were obtained when the reaction temperature was fixed at 50 °C and HNO_3 (1 M) was employed. The AHM solution containing 1 M of Mo, corresponding to sample 257, yielded the hexagonal phase. For 0.7 M of Mo, corresponding to sample 228, hexagonal MoO_3 was produced.

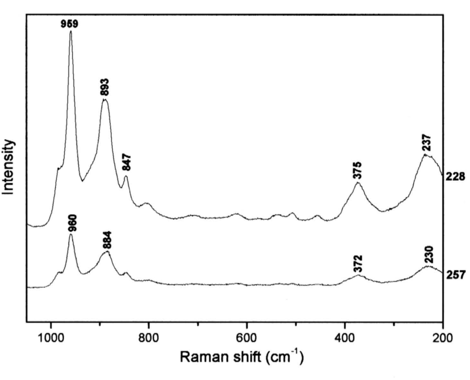

Fig 3.14 Raman spectrum of 2 samples prepared at the same concentration of HNO_3 (1.0 M) and temperature (50 °C) and varying AHM concentrations; sample 227: 0.7 M and 228: 1.0 M.

When the influence of the acid concentration was checked (1 M and 2 M HNO_3, 50 °C and 0.7 M AHM correspond to samples 227 and 225, respectively) again the XRD result was confirmed by Raman spectroscopy (see Figure B2). More figures with comparisons are attached in appendix B (Figure B6-B17).

Table 3.8 shows a summary of phase identification of all samples prepared using ammonium as counter-ion. The phase identifications are in good agreement and comparable with XRD investigations.

Tab 3.8 Raman phase identification of samples prepared using ammonium as counter-ion

Sample Name	**[Mo] (M)**	**[H$^+$] (M)**	**Temperature (°C)**	**Phase**
256	0.7	1	30	Supramolecular-like phase
227	0.7	1	50	Hexagonal molybdenum oxide
232	0.7	1	70	Hexagonal molybdenum oxide
257	1	1	30	Supramolecular-like phase
228	1	1	50	Supramolecular-like phase
258	1	5	30	Supramolecular-like phase
248	1	5	50	Hexagonal molybdenum oxide
225	0,7	2	50	Supramolecular-like phase
223	1	2	50	Supramolecular-like phase

The investigation of K as counter ion with Raman started with K_2MoO_4 at 0.28 M and HNO_3 at 2.0 M with reaction temperatures of 30, 50 and 70 °C. The product yielded at 30 °C with band positions at 963, 882, 373 and 229 cm^{-1} is assigned to the supramolecular phase. While at 50 and 70 °C, almost identical products with Raman band positions at 882, 904, 692, 496, 401 and 255 cm^{-1}, correspond to sample 249, 219 and 229 respectively (Figure 3.15) were obtained. These two phases show very similar bands shapes, shoulders and relative intensities in Raman Spectroscopy and is assigned to hexagonal MoO_3. The is in good agreement with the XRD investigation. In both cases additional heating was necessary.

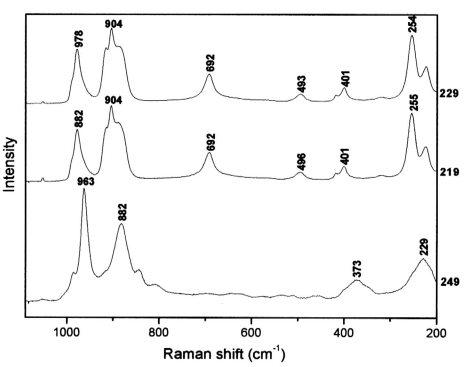

Fig 3.15 Raman spectrum of 3 samples prepared at the same concentration of K_2MoO_4 (0.28 M) and HNO_3 (2.0 M) and varying in temperature (sample 249:30 °C, 219:50 °C and 229:70 °C).

The situation is different when the molybdenum concentration is increased to 2 M as shown in Figure 3.16. At 30 °C (sample 250) a product was obtained by spontaneous precipitation. Bands are detected at 961, 898, 372 and 240 cm^{-1}. This is in line with the band positions reported for the $K_8Mo_{36}O_{112}$ compound [40]. However comparing the relative intensities of the band at 961 cm^{-1} to the band at 898 cm^{-1} the latter is slightly lower. For the Raman spectrum of the compound obtained at 50 °C (sample 245) the situation is similar.

The mismatch in band intensity is increased and bears close similarities with the motif of the hexagonal MoO_3 in this region. The spectra of the compound obtained at 70 °C (sample 244) is different. The main bands are observed at 949, 938, 909, 612, 372 and 217 cm^{-1}. Taking the intensity pattern into account, the compound can be identified as $K_2O * 3\ MoO_3 * 3\ H_2O$. However there is a slight, non systematic shift in band positions. In the literature a triad of very sharp bands were reported. This triad is not well resolved and a further shoulder is detected at 873 cm^{-1} which is not reported in the literature. The band detected at 1051 cm^{-1} is due to nitrate ion from the precipitating agent.

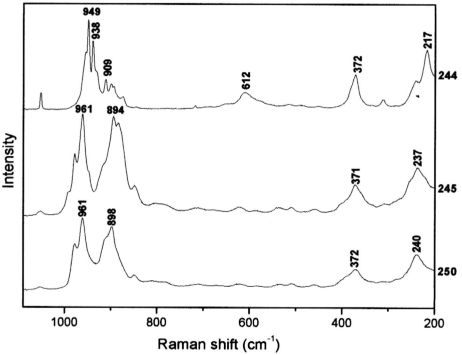

Fig 3.16 Raman spectrum of 3 samples prepared at the same concentration of K_2MoO_4 (2.0 M) and HNO_3 (2.0 M) and varying temperature (sample 250: 30 °C, 245: 50 °C and 244: 70°C).

Further samples with temperature variations were conducted by increasing the acid concentration to 5 M. The products obtained at 30 °C and at 50 °C are very similar to the previous experiment. The Raman trace of the trimolybdate however fits much better to the reference.

The influence of the molybdenum concentration was checked using the following parameters: temperature of 30 °C and HNO_3 of 2.0 M (Figure 3.17). The Mo concentration was increased from 0.28 M to 2 M. The samples were identified as $K_8Mo_{36}O_{112}$. In the first case the band at 882 cm^{-1} is slightly shifted to lower wavenumber as compared to the literature. In the second case the band positions fit exactly. Differences manifested in XRD are more severe.

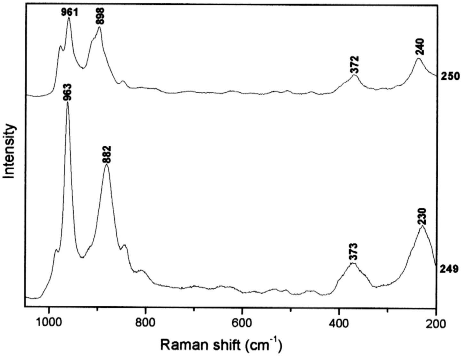

Fig 3.17 Raman spectrum of 2 samples prepared at the same concentration of HNO_3 (2.0 M) and temperature (30 °C) and varying K_2MoO_4 concentration (sample 249: 0.28 M and 250: 2.0 M).

At 50 °C the situation is different. Looking at the sample obtained from the solution containing 0.28 M all bands are in line with the one reported for hexagonal MoO_3. In the case of the 2 M concentration all band positions fit with the ones reported for the supramolecular phase. However the intensity of the band at 894 cm^{-1} is too high. The experiment carried out at 70 °C induces spontaneous precipitation. The sample with the low concentration of 0.28 M shows clearly the presence of hexagonal MoO_3 phase. The solution with higher solution concentration yielded basically trimolybdate. Sample 244 has been described earlier. Varying the acid concentration between 2 M and 5 M yielded again the supramolecular phase when K_2MoO_4 M was employed and experiment carried out at 30 °C. The first spectrum is described above. The second shows again a mismatch in band intensities and a shift. Table3.9 shows the overall results of phase obtained from potassium cation.

Tab 3.9 Phase identification of samples prepared using potassium as counter-ion

Sample Name	**[Mo] (M)**	**[H$^+$] (M)**	**Temperature (°C)**	**Phase**
249	0.28	2	30	Supramolecular like-phase
219	0.28	2	50	Hexagonal potassium molybdenum oxide
229	0.28	2	70	Hexagonal potassium molybdenum oxide
250	2	2	30	Supramolecular like-phase
245	2	2	50	Supramolecular like-phase
244	2	2	70	Trimolybdate
253	2	5	30	Supramolecular like-phase
246	2	5	50	Supramolecular like-phase
243	2	5	70	Trimolybdate
254	0.28	5	30	Supramolecular like-phase
247	0.28	5	50	Hexagonal potassium molybdenum oxide
233	0.28	5	70	Hexagonal potassium molybdenum oxide

Using Lithium as counter ion, bands are detected at 997, 825, 668, 376, 335, 292 and 244 cm^{-1}. This is in line with the bands reported in the literature [52] for orthorhombic MoO$_3$ apart from the band at 825 cm^{-1}, which should be at 820 cm^{-1}. Further a shoulder is detected at 980 cm^{-1}, which does not belong to MoO$_3$. All samples were prepared at the same concentration of Li$_2$MoO$_4$ (0.28 M) and titrated with HNO$_3$ (2.0 M) but at different temperatures of 30 °C, 50 °C and 70 °C correspond to sample 251, 222 and 230, respectively (Figure 3.18). XRD investigation also revealed orthorhombic phase structure.

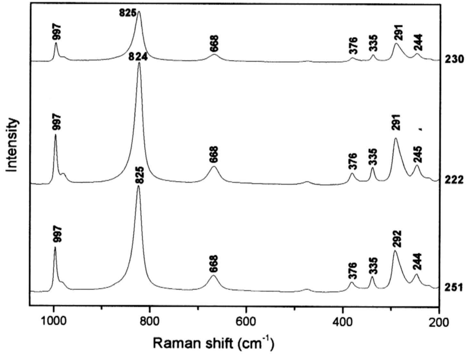

Fig 3.18 Raman spectrum of 3 samples prepared at the same concentration of Li$_2$MoO$_4$ (2.0 M) and HNO$_3$ (2.0 M) and varying temperature (sample 250: 30 °C, 245: 50 °C and 244: 70 °C).

Sodium (Na) counter ion sample shows good agreement with XRD data. The spectrum shows reflection pattern characteristic of hexagonal phase structure even though temperature was varied to 30 °C, 50 °C and 70 °C which correspond to sample 252, 256 and 231 (Figure 3.19). The spectrums are similar except differences in intensity.

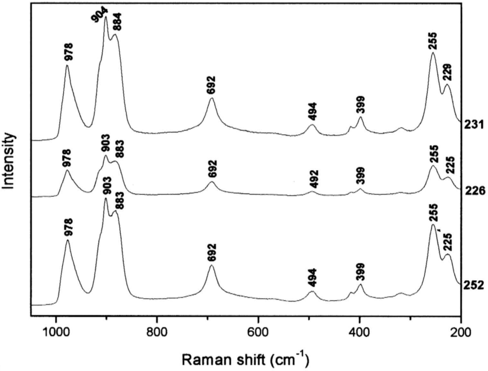

Fig 3.19 Raman spectrum of 3 samples prepared at the same concentration of Na_2MoO_4 (2.0 M) and HNO_3 (2.0 M) and varying temperature (sample 252: 30 °C, 226: 50 °C and 231: 70 °C).

Table 3.10 shows summary of phase identification by Raman spectroscopy for both lithium and sodium cations. The phase determination agreed well with XRD identification. All samples from these two cations did not precipitate in the solution at low temperature but need further heating. Even though both cations are from the same group of alkaline metal and need to be further heated, they yielded different type of phase structure, *i.e.* hexagonal and orthorhombic MoO_3.

Tab 3.10 Phase identification of samples prepared using lithium and sodium as counter ions.

Sample Name	**[Mo] (M)**	**[H^+] (M)**	**Temperature (°C)**	**Phase**
Lithium counter-ion				
0251	0.28	2	30	Orthorombic molybdenum trioxide
0222	0.28	2	50	Orthorombic molybdenum trioxide
0230	0.28	2	70	Orthorombic molybdenum trioxide
Sodium counter-ion				
0252	2	2	30 (further heated)	Hexagonal sodium molybdenum oxide
0226	2	2	50	Hexagonal sodium molybdenum oxide
0231	2	2	70	Hexagonal sodium molybdenum oxide
0255	2	5	30	Hexagonal sodium molybdenum oxide

3.3 Electron Microscopy (EM)

3.3.1 Transmission Electron Microscopy (TEM)

In this part, few interesting samples have been selected to be presented in the thesis. The selected samples were only obtained from ammonium cation. Ammonium has been chosen because it produced an interesting compound, *i.e.* Supramolecular $Mo_{36}O_{112}^{4-}$ which is believed to have a similar structure as MoVTeNb [63]. TEM is a suitable tool to investigate the microstructure of the compound.

Figure 3.36 A shows a high resolution Transmission Electron Micrograph (HRTEM) of the sample prepared at 0.4 M of Molybdenum and 1.0 M of HNO_3 from ammonium cation (Sample 1). XRD and Raman Spectroscopy investigated the phase as supramolecular $Mo_{36}O_{112}^{4-}$. Figure 3.36 A is a projection of at least 4 overlapping particles. Both well-developed crystals and non-crystalline particles are revealed in the images. The lines in Figure 3.36A are outlines of different particles. The crystalline areas reveal nice lattice fringes. However, contrast variations (light and dark) are observed due to thickness effects and overlapping features. Figure 3.36 B shows Fourier Transform of crystalline area from Figure 3.36 A. The diffraction spots correspond to lattice spacing of 5.58 Å and 3.11 Å with an angle of 88 °. The spots are distinct and bright.

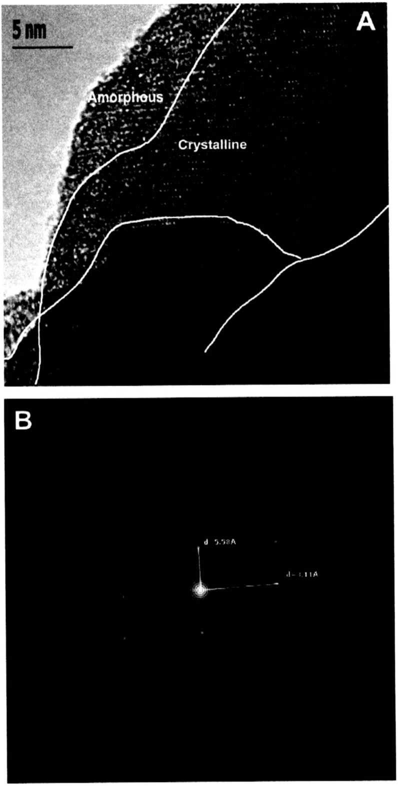

Figure 3.36. High resolution image and Fourier Transform of the crystalline part of samples prepared by decreasing pH (acid concentration: 0.4 M) from ammonium cation (sample 1).

Figure 3.37 shows a comparison of XRD pattern with d-spacing observed in HRTEM images. The lattice spacings are calculated from approximately 30 lattice fringes images. HRTEM is not suited for quantitative measurements of the lattice spacings, so the observed lattice spacing is considered qualitatively. The XRD pattern has much more intense peak at low angle which does not fit well with HRTEM investigation. On the other hand, the small peaks with low intensity of XRD patterns agreed reasonably well with the HRTEM investigation. The d-spacing calculated from the HRTEM images correspond to 5.58 Å while the value is 1.9 nm as investigated by XRD.

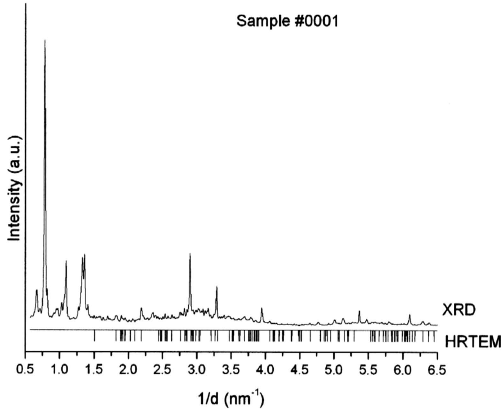

Fig. 3.37 Supramolecular structure revealed from XRD and TEM investigation, plot of intensity as a function of d-spacing (sample 1).

Figure 3.38 shows an electron micrograph and HRTEM images of sample prepared at 1.0 M acid concentration from ammonium cation. Two types of particle size distribution are observed, one with small particle size (circle mark) and one with big particle size (arrow). The big particles have a particle size distribution range of 2-3 μm. The small particles are smaller than 100 nm. The small particle is better suited for HRTEM than the big particles. The HRTEM image in Figure 3.38 B shows different orientation and arrangement of lattice fringes representing d-spacings of range 3.7-3.8 Å. The edge of the particle is amorphous at approximately 2.5 nm distances.

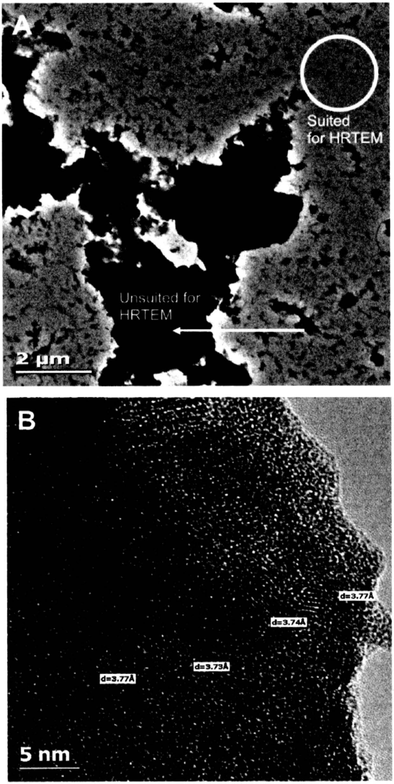

Figure 3.38. Electron micrograph and HRTEM image of samples prepared by decreasing pH (varied acid concentration at 1.0 M) from ammonium cation (sample 5).

Figure 3.39 A shows a big particle with approximately 400 nm in size. The particles are built in layers which are agglomerated to form a huge particle. Figure 3.39 B is the corresponding Selected Area Electron Diffraction (SAED) taken from A. The SAED pattern shows diffuse rings without any bright and distinct spots. However, HRTEM images in C which have been marked with two circles, indicates some kind of fringes in a very small area (size of the circle). The surrounding area shows no arrangement of lattice fringes not only at the edges but in the inner part too.

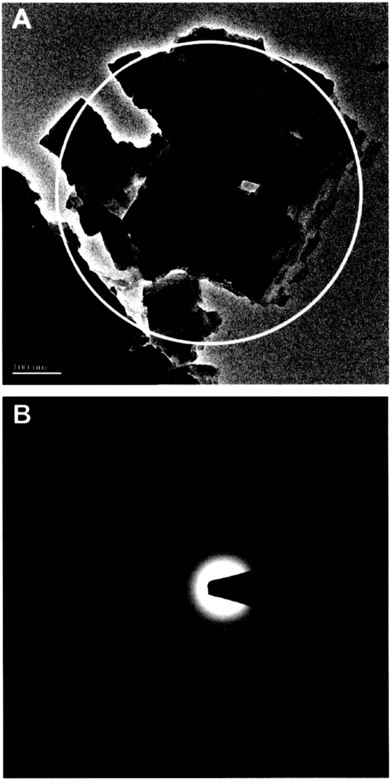
A
100 nm
B

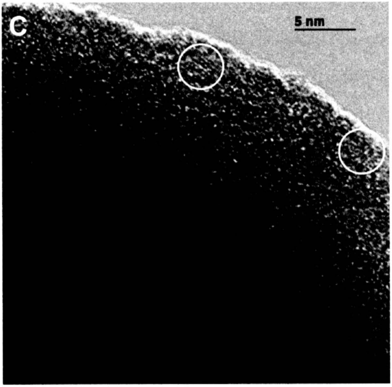

Figure 3.39 Electron micrograph, SAED, and HRTEM of samples prepared at varying temperature (30 °C) from ammonium cation (sample 256).

Figure 3.40 shows images of sample 227 prepared at temperature of 50 °C from ammonium cation, higher temperature was applied compared to sample 256 which was prepared at 30 °C. Figure 3.40 A shows an electron micrograph indicating the distribution of two significant types of particles, one type with very small particle size and the other type with a very big particle size. The size of the biggest particle is approximately 2 μm. HRTEM images have been acquired from the small particle which can be seen in Figure 3.40 B. Two circles marked in the HRTEM image to show two different particles which are the same size as the circle, both with different lattice fringes. The d-spacing for both marked lattice fringes are 3.4 Å and 3.8 Å. Figure 3.40 C and D show an electron micrograph and electron diffraction pattern of the same sample. From the distinct pattern in Figure 3.40 D it can be deduced that the big particle in Figure 3.40 C (approximately 200 nm) are one single crystal. The distinct spots in the electron diffraction pattern corresponds to 3.3 Å and 3.9 Å separated by an angle of 79°.

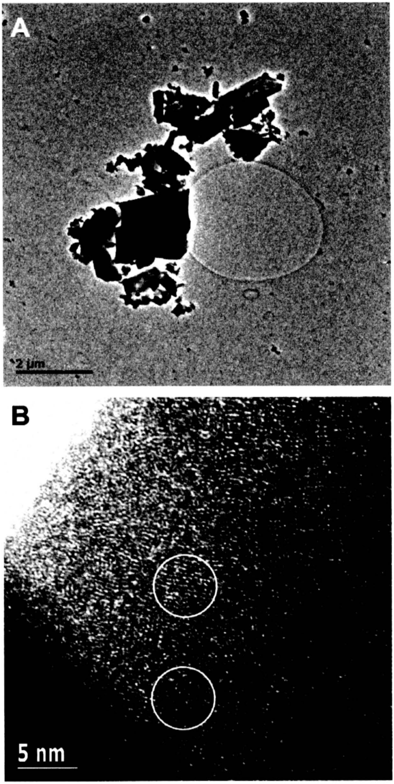
A
2 µm
B
5 nm

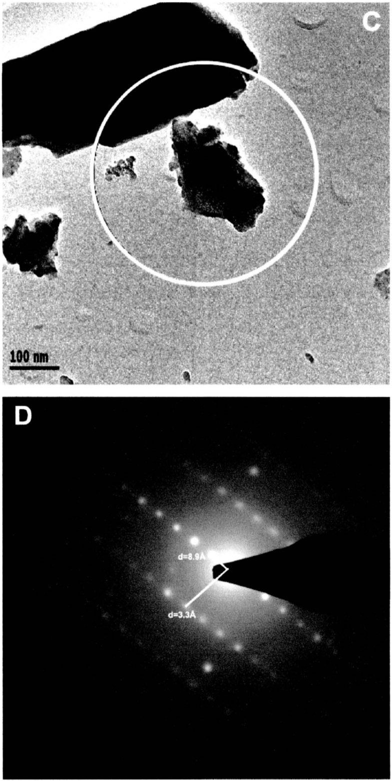

Fig 3.40 Electron micrograph, electron diffraction pattern and HRTEM images of samples prepared at varying temperature (50 °C) from ammonium cation (sample 227).

Figure 3.41 shows images of an electron micrograph, electron diffraction pattern of ammonium samples prepared by varying temperature (70 °C). The electron micrograph reveals a bigger and better developed crystal compared to crystals observed in Figure 3.40. The particles are agglomerated and overlapped to each other with different d-spacings, 3.22 Å and 3.33 Å. Again there are bigger and smaller particles. The big particles have sizes between 6-7 μm while the small particles are typically less than 1 μm. Even the shapes of both small and big particle are totally different. The big particles have a well defined surface or facets. Electron diffraction pattern shows distinct and bright spots with d-spacing 3.3 Å and angle 70 °.

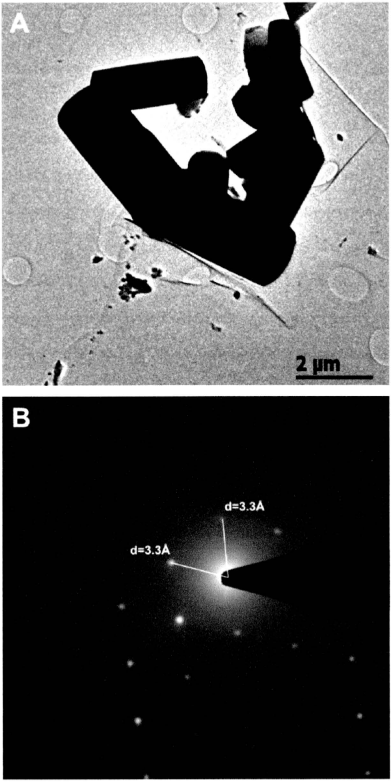

Fig 3.41 Electron micrograph and Electron diffraction of samples prepared by varied temperature (70 °C) from ammonium cation (232).

3.3.2 Scanning Electron Microscopy (SEM) and Energy Dispersive X-ray (EDX)

Figure 3.26 shows SEM images of the samples prepared at two different acid concentrations namely the highest (1.0 M) and the lowest (0.4 M). The first image (on the left) (sample 5) was prepared at 1.0 M acid concentration while the second image (sample 1) was prepared at 0.4 M acid concentration. Sample 5 has a rod-like particle shape mostly and small particles without any special shape. The big particles with rectangular-like shape are about 5 μm size and the small particles have size approximately of 1 μm. The surfaces of the particles are smooth and some of the particles look like layers. Sample 1 (0.4 M acid concentration) have particle size in the range 5-6 μm. The shapes of the particles have less rectangular-like shape. The particles without any special shape are more predominant than the rectangular-like particle. EDX analysis at various position showed that the atomic ratio of Mo:O is approximately 80:20. There were no real differences in the atomic ratio of all samples of variable acid concentration from the highest acid concentrations to the lower acid concentration.

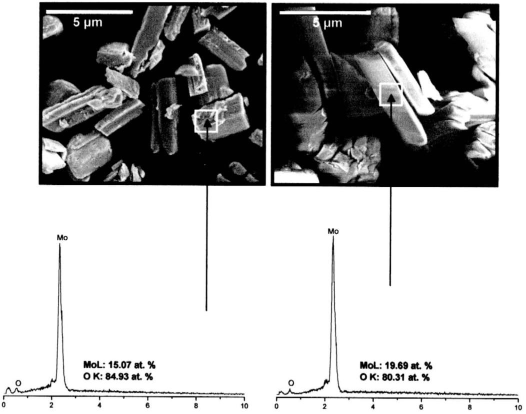

Fig. 3.26 SEM images of samples prepared by varying acid concentration; sample 5 (1.0 M, on the left) and sample 1 (0.4 M, on the right).

Figure 3.27 shows SEM images of samples prepared by different temperature. Sample 256 was prepared at temperature 30 °C while sample 232 was prepared at temperature 70 °C. Other parameters were fixed for instance, the acid and molybdenum concentration in the solution sample. The first image which corresponds to sample 256 has a rectangular-like shape with size ranges from 6 to 8 µm. Some of the particles are small with size of 1-2 µm without any special shape. The surfaces of the particles are smooth and consist of layers. The second image which corresponds to sample 232 has hexagonal shape particles. The surfaces of the particles are really smooth without any layers. Parts of the hexagonal particles are single particles and some of them agglomerates together which look like flowers. The lengths of the hexagonal particles are in the order of 2-3 µm. EDX analysis of this characteristic sample showed that the atomic ratio of Mo:O is about 80:20. The atomic ratios of all positions measured are almost similar.

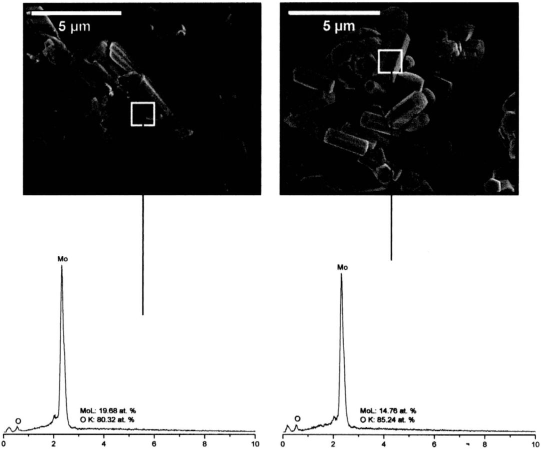

Fig 3.27 SEM images of samples prepared by varying temperature; sample 256 (30 °C, on the left) and sample 232 (70 °C, on the right).